Int. J. Nonlinear Anal. Appl. 14 (2023) 1, 1671–1682
ISSN: 2008-6822 (electronic)
http://dx.doi.org/10.22075/ijnaa.2022.27660.3672

A hybrid approach of dynamic image processing and complex network to identify repetitive images of welding defects in radiographs of oil and gas pipelines

Ali Ebrahimi[a], Kamal Mirzaie[a,*], Ali Mohamad Latif[b]

[a]Department of Computer Engineering, Maybod Branch, Islamic Azad University, Maybod, Iran

[b]Department of Computer Engineering, Yazd University, Yazd, Iran

(Communicated by Javad Vahidi)

Abstract

Pipelines are the safest as well as the most economical way to transport gas and condensate over long distances. Radiographic images are provided to commentators as a tool to diagnose welding defects in metal lines, so the study of welding in gas and oil pipelines has always been one of the most important areas of non-destructive testing. Expert interpreters are now used in many countries to interpret radiographic films from non-destructive tests. Interpreters can detect the number of pores on the weld surface by viewing radiographic images due to the limited number of these people and their unavailability. In some cases, there are many problems. For human interpretation, radiographic videos must be collected and sent to the interpreter's place of work or residence. The purpose of this article is to provide a method that can be used to interpret radiographic films quickly using conventional image processing methods and identify the welding defects in them and determine whether these defects are duplicates or not. The method of image segmentation is the area growth method. The main feature of this method is its proper performance in images such as radiographic images that have less subject variety. This method separates a part of the image from the rest by determining a pixel in the image as the starting point and expanding the area around this point due to the similarity between the pixels. In this paper, based on the histogram, the start and end image of the welding range is determined automatically. Then a combination of different standard algorithms is applied to identify defects in the image. Then, the key points of the image are extracted, and using them, the corresponding complex dynamic network is drawn and its calculations are performed. The simulation results show that the proposed method covers the shortcomings of the previous methods and in addition to bringing the detection of welding defects by computer closer to human diagnosis and in some cases works better than human performance, it has also made it possible to identify duplicate images.

Keywords: Welding defects, Radiography, Image processing, Non-destructive tests, Dynamic complex network, Network similarity
2020 MSC: 68U10, 68M15

*Corresponding author
Email addresses: ebrahimi@nigc-yazd.ir (Ali Ebrahimi), k.mirzaie@maybodiau.ac.ir (Kamal Mirzaie), alatif@yazd.ac.ir (Ali Mohamad Latif)

Received: May 2022 *Accepted:* July 2022

1 Introduction

At early 1920s, one of the initial applications of digital photography was in the newspaper industry. Bertlan photo-transfer service cable transferred images between London and New York through the sea. The images were codified for transfer and at target; they were decoded on a telegraph printer [3] (Fig. 1). This system was upgraded over the years to produce higher quality images. In the 1960s, advances in technology computing and the beginning of a competitive environment led to a wave of work in digital image processing.

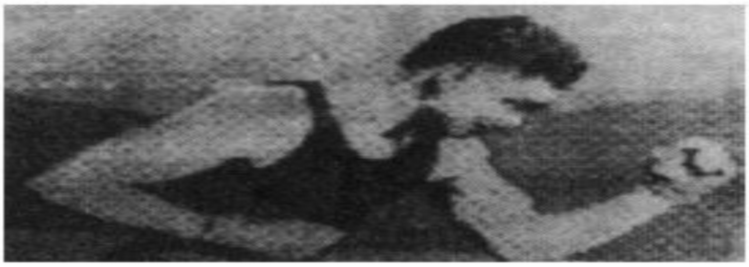

Figure 1: The first digital image that was published in 1921 by a telegraphic printer

From the early 1980s until today, the use of digital image processing techniques has been increased and currently these techniques are used for any kind of work. In 1990, Hubble telescope could take pictures of objects far away. However, a false reflection made useless a large number of images sent by Hubble. It was this time that image-processing techniques were built to be used to reconstruct the images.

2 Statement of the problem and the necessity of the research

Typically for each application in machine vision, an image segmentation phase is first performed. In output of this step, each object in the image is represented by a set of pixels. The purpose of this stage is that the objects and the backgrounds are separated except the sets that are overlapping. Image segmentation is generally based on two characteristics of light intensity and similarity. Methods proposed for segmenting images separate the objects in the image based on one of these two characteristics or a combination of them. For segmenting images, one of the following ways that are proposed in continuation can be used.

The first way studied is the threshold limit. This method works in this way that by setting a threshold value, the values higher than the threshold limit are considered as an object and the lower values are considered as another object. The key point in this method is to determine the threshold limit. In the method, multilevel threshold limit can also be used. Threshold limit method is a simple method, which is used for optimized images that do not include a lot of objects [2]. Histogram method is also one of the methods for image segmentation. In this method, a histogram of all pixels in the image is calculated and the ups and downs in the histogram are used for image segmentation [14]. The color or intensity of light can be used for measurement. The implication of this method is that the image is divided into clusters using the ups and downs of the histogram. The disadvantage of histogram method is that the identification of the ups and downs in the image may be difficult [14]. Edge detection method is also one of the methods for segmenting images. In this method, the boundary of the objects is detected using rapid changes in brightness intensity or color of the pixels. By detecting these borders, segmentation can be done in the best way [1]. Region growing method is also another method for segmenting images. In general, the way of its working is so that by determining a seed (starting point), the surrounding points are compared with the mean of the seed and other points of the region and in the case of having required similarity are considered as that region. The main problem of this method is that the seed must be determined manually, which prevents its automatic function. Another problem is that the noise severely influences its performance [7]. This paper attempts to invent a combination method, which has the best efficacy for welding radiographic images by precisely investigating the algorithms that are subset of one or a combination of the mentioned methods.

3 Basic concepts of image processing and review of research

Images from digital devices have always had a noticeable amount of noise or blur, and in some cases have the problem of blurring the boundaries inside the image, which reduces the sharpness of the received image. Image processing science is one of the most widely used and useful sciences in the industry. Pixel is the smallest element of the displaying or printing hardware and software used to form images. If only two colors (usually black and white) are considered for each pixel, that pixel can be coded by a single bit of information, and if more than two bits are used to represent a pixel, a wider range of colors or gray shades can be provided. The greater the number of bits used to represent a point, the more the colors and gray shades we can represent. The density determines the dots or resolution of the image. We measure this feature by unit of dot per inch (DPI) or by the number of rows and columns, e.g., 640×480. An image can be shown by a two-dimensional function of $f(x, y)$, where x and y are called local coordinates and the value of f at each point is called the intensity of image resolution at that point. The term 'gray level' also refers to the resolution intensity of monochromic images. Color images also consist of a number of two-dimensional images. When the values of x and y and the value of $f(x, y)$ are expressed by discrete and finite values, the image is called a digital image. To display an $M \times N$ image, a two-dimensional matrix with M rows and N columns is used. The value of each element of the matrix represents the intensity of image resolution at that point. Each matrix element is an 8-bit value that can have a value between 0 and 255. Zero represents the dark color (black) and the value 255 represents the light color (white). For example, in figure 2, we have used a matrix with 256 rows and 256 columns to display the image. Each pixel of the image has a value between 0 and 255. All functions of image processing use these values and apply necessary actions on the image [8]. Separation of two images with the same size means that we subtract the resolution density of corresponding pixels of the images from each other. When subtracting the pixel values, we convert negative values to zero. Adding two images means that we add the intensity of corresponding pixels in two images to each other. One of the most common applications of adding two images is to add a background to the image.

Suppose we have several identical images with different noises on each of them and we want to improve the quality of these images. In such cases, we can use the averaging of all images, so that we sum the values of the corresponding pixels in all images and then divide it into the total number of images. Obviously, the more the number of images for averaging, the closer to reality the resulted image from their averaging will be [8].

Figure 2: The gray level image

One of the useful features of the object recognition is to use the image information and its edges. Therefore, the use of edges in many machine vision applications and recognition is common. Various algorithms have been developed and proposed for detection. In classical methods of edge detection, we consider local maximums of image gradient as the appropriate representative for the edges. Robert, Sobel detectors belong to this category. Of other efficient algorithms in this field is Canny edge-detector, which is very applicable due to having the capability of following the edge and removing the image noise by Gaussian filter [9]. Image histogram is a graph by which the number of pixels of each level of brightness is specified in the input image. Suppose the input image is a gray level image with 256 brightness levels, so each pixel of image can have a value in the range of 0 to 255. To get the image histogram, it is enough to calculate the number of pixels in each brightness level by measuring all p pixels of the image. We can also achieve normal histogram by dividing the values of the histogram into the total number of image pixels. Normalization of the histogram causes the histogram values to be set in the range. Figure 3 shows an image with the normalized histogram.

One of the applications of histogram is in the autofocus of digital cameras, in a way that the camera lens moves from beginning to end and at each step of its motion takes a picture of the scene. Then, it calculates the contrast of the taken image using its histogram. Once the lens reaches the end of its motion, some point of lens motion where the image has had the highest contrast is determined as the locus of lens. This method is one of the simplest ways of autofocus of camera and as we can guess this algorithm will have some drawbacks in the scenes, that there are dark and bright colors together, and we have to apply some changes in it [9].

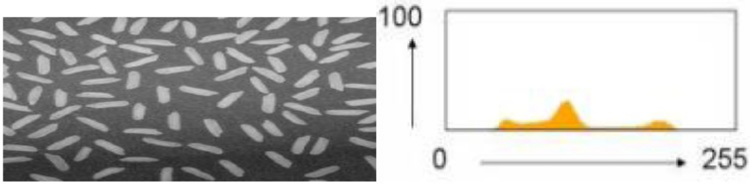

Figure 3: An image with the normalized histogram

Another usage of histogram is to increase the contrast in images with low contrast. When we say the image contrast is low, it means that the difference between the minimum and maximum image brightness is low [9].

Histogram equalization causes the contrast of the input image increase as much as possible. For example, Figure 4 and figure 5 shows an image before and after histogram equalization.

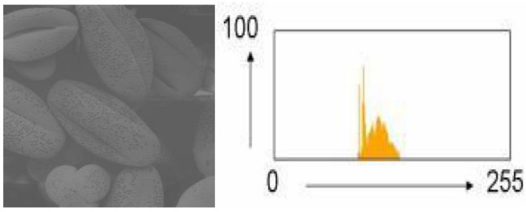

Figure 4: Image before histogram equalization

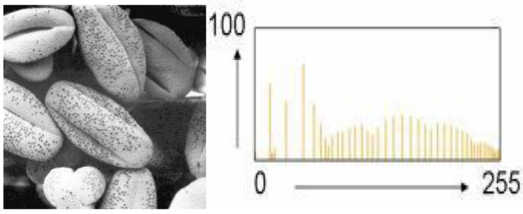

Figure 5: Image after histogram equalization

4 Basic Concepts of Complex Networks

A complex network, a graph with a set of vertices connected by edges. Complex networks can be classified into three main models: 1- Random networks 2- Small world networks 3- scale Free networks. In the random networks, which is the simplest model, the edges are added randomly. Each complex network has a specific topological design that determines how it is connected. Therefore, the analysis of complex networks depends on the use of measurements, which leads to the extraction of appropriate topological designs and their classification. Grade distribution is an important attribute of the vertex in the graph. Given vertex degrees, many measures can be formulated, with the two most straightforward measurement techniques as seen in (4.1) and (4.2):

$$K_{\max} = \max_i K_i \tag{4.1}$$

$$K_{avg} = \frac{1}{n} \sum_{i=1}^{n} K_i \tag{4.2}$$

where K_i indicates the degree of node i. Structural and dynamic networks can be principally characterized by connectivity degree distribution, including: i) entropy, ii) energy, and iii) average connection degree.

The entropy of connectivity degree distribution can be determined as seen in (4.3):

$$K_{jd}(k,k') = -\sum_{k,k'=1}^{K_{\max}} p(k,k')\log(p(k,k')) \tag{4.3}$$

the normal distribution-associated energy can be determined as seen in (4.4):

$$E = \sum_{k,k'=1}^{K_{\max}} p(k,k') \tag{4.4}$$

one way to detect the loop is through the clustering coefficient, which is beneficial for network analysis like degree. Two different clustering coefficients are typically used, the first of which, according to the definition of non-directional networks, is as follows:

$$E = \frac{3N_{\Delta}}{N_3} \tag{4.5}$$

where N_{Δ} represents the number of triangles on the grid and N_3 represents the triangles.

A triangle has three vertices, with an edge between each pair, a triangular connected set of three vertices, whose two vertices are adjacent to a third one (i.e., central vertex). Clustering factors can be obtained for a grid by calculating the mean clustering factor for each vertex. The clustering factor of vertex i can be measured as follows:

$$C_i = \frac{N_{\Delta}(i)}{N_3(i)} \tag{4.6}$$

where, $N_{\Delta}(i)$ denotes the number of triangles with vertices i and $N_3(i)$) denotes the number of triangles, i.e., the central vertex. The clustering coefficient of a network can be defined as follows:

$$\overline{C} = \frac{1}{N}\sum_i C_i \tag{4.7}$$

the distance is an important size, depending on the overall network structure. We can measure the network as the mean of the shortest distance by calculating the mean distance of the shortest line (path) for each pair of vertices, such as the following formula:

$$d_G = \frac{1}{N(N-1)}\sum_{i+j} d_{ij} \tag{4.8}$$

d_{ij} represents the shortest line distance from vertex i and vertex j.

Assume graph $G=(V,E)$. Here, E and V indicate the set of edges and vertices, respectively. $|E|$ and $|V|$ denote the number of edges and nodes of the graph G, respectively. The network model can be defined as $GN=(V_N,E_N)$ for the G graph. Each edge of the graph G is a vertex GN. The weighting vector for each vertex can be measured by evaluating the relationship between and geometric position of the edges, as shown in Figure 6, the weighting vector for vertex i can be measured as seen in (4.9):

$$e_i = (l_i, d_i, d_{1i}, d_{2i}, x_i, y_i) \tag{4.9}$$

where l_i represents edge length, d_i represents the distance between the edge center and graph center (Point o), d_{2i} and d_{1i} the intervals from the beginning of the edge to the center of the graph (point o) and from edge end to graph center (point o) and x_i and y_i are the center point coordination of the edges.

The network is formed by a set of non-directional edges E that connects each pair of vertices. The value of the edge of vertex i to vertex j can be calculated using the Euclidean distance between e_i and e_j:

$$W_{ij} = d(e_i, e_j) \tag{4.10}$$

therefore, the network can be mapped as $|E|\times|E|$ and show the weight w with the matrix.

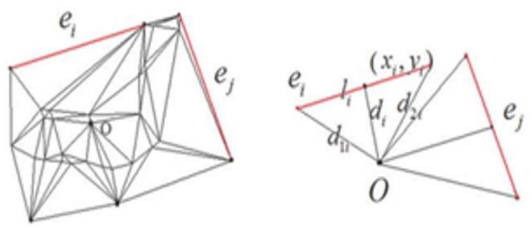

Figure 6: Schematic representation of a graph based on a complex network

$$W_ij = W([e_i, e_j]) \tag{4.11}$$

and then normalize it to form:

$$W = \frac{W}{\max(w_{ij} \in W)}. \tag{4.12}$$

The network model $GN = (V_N, E_N)$ is initially a regular network that connects the set of edges of E_N to each node of the network; although however, this regular network does not offer any good useful features for the program. Hence, this regular network must be transformed into a complex network with appropriate characteristics. Here we carry this transition using the method applied in [17] and define the threshold t. This transition is performed to create a new edge set for the network by choosing a subset of performed the $\hat{E}_N$ of E_N which eliminates the need for the edges of the E_N to have a lower weight than the threshold of t. This can be defined as:

$$G^t_{CN} = \delta(G_N, t) = \begin{cases} w_{ij} = 0 & if\ w_{ij} \geq t \\ w_{ij} = 1 & if\ w_{ij} < t \end{cases} \tag{4.13}$$

where t varies between t_0 and t_f and the first and final thresholds (t_f, t_0) are user-defined. Given a graph $G = (V, E)$, we first model the graph structure using network G_N and then extract measurements from networks G^t_{CN} by varying the threshold t. Afterwards, our CNCRG is performed as the concatenation of these measurements. Three distinct feature vectors are proposed, i.e., degree descriptors, joint degree descriptors, and clustering-distance descriptors. Using formulas described in (4.1)-(4.3), φ_t denote degree descriptors as follows:

$$\varphi_t = (K_{\max}(t), K_{avg}(t), K_d(t)) \tag{4.14}$$

using formulas described in (4.3) and (4.4), γ_t denote joint degree descriptors as follows:

$$\gamma_t = (H_{jd}(t), E_{jd}(t)) \tag{4.15}$$

using formulas described in (4.7) and (4.8), ξ_t denote clustering-distance as follows:

$$\xi_t = (\overline{C}(t), G_d(t)) \tag{4.16}$$

the final feature vector for G^t_{CN} can be computed as:

$$f_t = [\varphi_t, \gamma_t, \xi_t] \tag{4.17}$$

with the feature vector for G^t_{CN} our CNCRG can be computed as the concatenation of f_t at different stages of the evolution of the network, according to the following:

$$CNCRG = f_{t0}, f_{t1}, ..., f_{tj} \tag{4.18}$$

this approach is used to convert the regular network to the complex network, as illustrated in Figure 7.

In [13], they showed the complex network $G^{t_0}_{c_n}$ is as suitable for the small-world model. This complex network model has two main characteristics: i) high clustering coefficient and ii) small-world property that can be based on the discussed issues. The clustering coefficients listed in (4.7) can be used to evaluate the characteristics of high clustering coefficients. The small-world property is quantified based on whether an average shortest distance is present on the network (4.8).

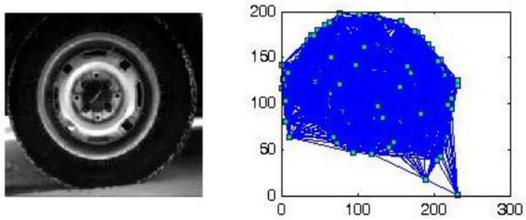

Figure 7: The image of a shape and its complex network

5 Background research

Weld quality interpretation is performed using a variety of non-destructive tests. Although image interpretation experts are in many cases better than machines in terms of image interpretation and quality control, but it gets tired very quickly and the process of interpretation and eventually done with delay.

Interpreting welding defects is a difficult task for people when a large number of welds have to be counted and interpreted. Many stages of interpretation seem time consuming and tedious to commentators. According to research, human efficiency in visual interpretation is as much as 10% of the energy and cost of mechanized systems [4]. In addition, developing and expanding the skills of interpreters through their training is difficult and time consuming. Therefore, in such situations, the use of mechanized interpretations is a good alternative for commentators. NDT include methods for detecting defects in objects without altering the object. Valid identification of welding defects is one of the most important tasks in non-destructive tests. Since the human factor still has a significant impact on evaluations, it is necessary to improve these methods.

Welding is one of the main processes for connecting and constructing many works of art and designed structures such as cars, ships, airplanes and spaceships, as well as oil and gas pipelines [12]. In [16] introduced an automated imaging system for the detection and evaluation of welding defects in gas pipelines using radiographic films. This imaging system, which is used to capture radiographic films, can be used to process various images and computer algorithms to identify welding defects and calculate the necessary information. They have introduced another imaging system that uses a variety of image processing and computer imaging algorithms to image radiographic films to identify defects and make decisions to accept them in accordance with international standards. This system is able to detect and test the main types of welding defects for welded gas pipelines that have a coating and are also protected. On the other hand, developments in image processing, computer imaging, artificial intelligence, and other fields have dramatically improved the efficiency of visual interpretation techniques. The advantage of image digitization is that it describes the object numerically, thus providing a selection of good features for the success of algorithms. In general, two-dimensional properties are computationally simpler than three-dimensional properties [11].

Jagannathan [10] introduced a new system for interpreting images of mechanized devices in corrugated soldered areas. Using this technique, an intelligent histogram is obtained from the gray surface of the histogram of images and divides the connections through various methods, and finally uses neural networks to identify and classify defective soldered connections.

6 Description of the Problem

The large number of radiographic images of long-distance pipelines makes it difficult and time consuming to identify welding defects. The most difficult issue in the interpretation cycle is the accurate identification of errors in radiographic images. Human interpretation in radiographic films is difficult when a large number of defects are counted and evaluated.

Obviously, different experts do not have the same ideas about a particular film, and even one expert may have a different idea about a film at the beginning and the end of the day. In general, the traditional method of interpreting movies has the following advantages and disadvantages:

Advantages of traditional system

- The interpretation cost of each film through current system is less than that of mechanized system.
- It is possible to employ the interpreter person at any place (no electric power and special equipment is needed).

- The interpreter is able to explain about the image and its defects.
- In low quality images, the experience of the interpreter can help him in detecting defects.

Disadvantages of the current method

- The cost of training interpreters of the images is too high.
- Development of the interpreters' skills through their training is difficult and time-consuming.
- The interpreter person gets tired during the interpretation process.
- The interpretation process of images by interpreters is slow and time-consuming.
- Interpretation of radiography films with low quality is impossible.
- The efficacy of interpreter and correct interpretation is higher in initial hours of work than the last hours.
- The interpretation is a difficult task when a lot of welds must be counted and interpreted.
- Sometimes the interpretations of an interpreter are different at the beginning and end of office hours (human error).
- Sometimes different interpreters have different ideas about interpretation of a single film.

In this section, we will introduce a new automated imaging system to identify and evaluate repetitive images of welding defects in gas pipelines by examining radiographic films. Radiographic films of welded pipelines are produced by radiographic test (RT) method. This method is based on recording different amounts of radiation absorbed by conventional radiographic films. These different values of absorption produce an image of the object on the film. The film is chemically modified to identify the inside and outside of the object. This film is called a radiographic film. If the object being tested by radiography (RT) is defective, more radiation will pass through the defective area than other areas of the film. The generated radiographs can be interpreted and their integrity can be assessed by an interpreter or automated interpretation system. When radiographic films are produced, the image quality indicators (IQI) are matched to the radiographic films to obtain quantitative information about the sensitivity of the produced films. Image quality indicators are test cables that accurately control dimensions and are produced from the same type of material used for radiography. The sensitivity of image quality indicators is usually measured based on the minimum size of visible cable relative to the thickness of the weld metal. The radiographic films used in this work are obtained from the projects of provincial gas companies and technical consulting companies in Iran. Radiographic films are based on the API 1104 standard, which is made of Iridium 192 (Ir-192), which is produced to meet the desired quality level.

In similar works, a camera and a moving table with several controllers and a microprocessor have been used to identify defects in the soldered areas [10]. The piece is placed on the table and different images are taken by moving the table in front of the camera. The image information is then transmitted to the computer via the RS232 port. Neural networks have been used to identify defects. To do this, a number of images are used to train the network and the system identifies defects based on the images.

In the system proposed in [15], the apparent defects of the weld (outer surface) have also been studied. For this purpose, 4 LED lighting areas with different angles are photographed from the welded place. Weld's are classified into 4 different groups including: acceptable, incomplete weld, excess weld and no weld. To identify defects, 80 different images (20 images per group) have been used to train the neural network. Then the system performance was examined using another 80 images which in 95% of cases the system performance was confirmed.

7 Research Method

The aim of this study is to provide a system for detecting defects in metal pipelines using radiographic films. This system, compared to the system provided by Shafeek et al [16], is applicable on any operating system and uses standard algorithms for image processing. In addition, to detect defects and dimensions of radiographic films, it does not require creating windows and getting additional information from the user. In this system, the dimensions of the film are not important and the system automatically recognizes the weld area, that is, this system is used for each type of film. To identify the boundaries of the welding, image histogram is used and the weld zone is easily identifiable. To detect defects and enhance image quality, the standard algorithms are used.

Harris algorithm is used to identify the edges and the resulting dynamic network is drawn based on the extracted key points [6]. Then the triangles are calculated and the corresponding graph is generated based on it. Finally, by using the features of complex networks and extracting them, similarities between images are obtained and similar images can be identified.

Similar to the system, we have used the ideas of the expert of film interpreter to test the system and the system performance has been tested based on his idea on 400 different films with different light intensities [5]. In addition, the provided system fixes the lack of details that have been caused due to darkness of the film, which its cause is the lack of storage of films on magnetic tools. Also there is the possibility of saving images resulting from processing, and there is no need to reprocess the images in reviewing the images. The provided visual system includes two parts: hardware and software. The hardware consists of a conventional computer with Windows 10 operating system and also a digital camera and a light table. The software used is 2018 version of MATLAB software to detect and evaluate defects in radiographic film of gas pipelines.

In addition, this software supports a great variety of image formats, such as: BMP, TIFF, GIF, JPG, PCX, and TGA. Work stages are as follows:

1. Radiographic film is placed on the light table.
2. The image is captured and saved by a digital camera.
3. The image is transmitted to the computer using the interface software and saved as a BMP format file.
4. The file is opened by MATLAB software and converted to a gray image.
5. The weld zone is identified, and then the various algorithms are respectively used to detect defects.
6. The edges of the defective area are identified.
7. A complex network is created from the edges.
8. The triangles obtained from the neighboring nodes are identified.
9. Dynamic network specifications are extracted based on the graph of the previous step.
10. Based on the information of the previous step and comparing them with each other, similar images are identified and categorized.

Many parameters such as lens focal distance, lighting conditions, and the focus on the quality of the recorded images are influential. To obtain high-quality images, the radiographic films should be recorded under optimal conditions. IQI produced on the radiographic films are considered as an optimum target for evaluating the obtained image quality. Therefore, the conditions of record should be adjusted so that each IQI characteristic can be clearly seen on radiographic films.

Here are many image processing algorithms in MATLAB software which can be used in radiographic recorded images to detect weld defects and to extract useful information from them. Figure 8 shows a diagram of the basic algorithms used in MATLAB software. As it is clear in figure, these algorithms are used in the order they have shown.

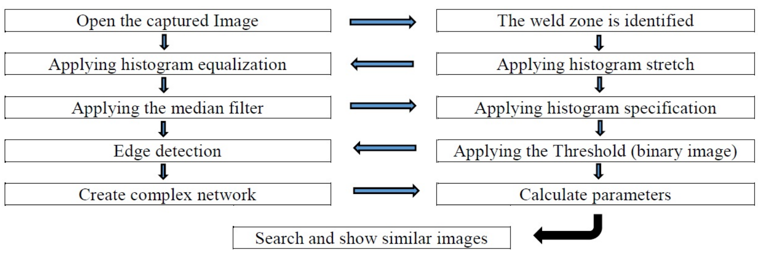

Figure 8: Identification diagram of similar images

8 Simulation and analysis results

As shown in figure 9 to 15, a special radiographic film AGFA (the reference of weld radiographic interpretation) is used for testing. Approaches to identify similar images have been shown in the figure 8. Figure 11 shows a special window after using histogram stretching algorithm surrounding the whole weld zone. In this image, the form of weld surface is improved and the two defects seem darker. As it is seen in figure 12, further improvement is obtained by using the algorithm of the equivalent histogram. In Figure 13, the image intermediate filter is used, so the image seems smoother than figure 12. In figure 14, the histogram specification algorithm has been used and defects are more obvious. Figure 15 shows the binary image of weld zone after using the threshold calculation.

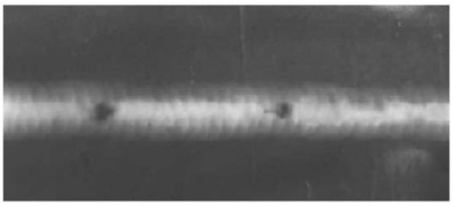

Figure 9: Captured radiographic image

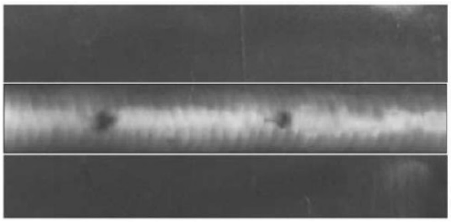

Figure 10: Specified window around the whole welding area

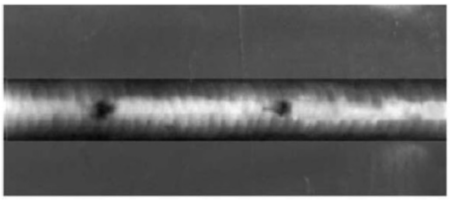

Figure 11: Applying histogram stretch

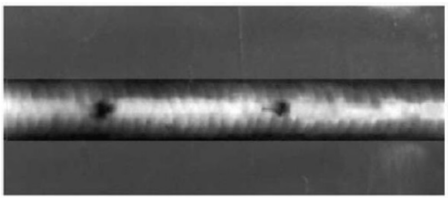

Figure 12: Applying histogram equalization

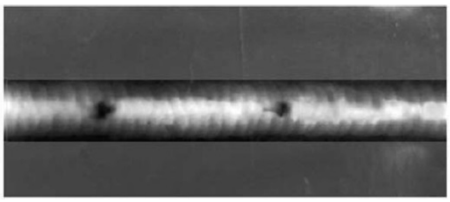

Figure 13: Applying the median filter

9 Conclusion and suggestion

Separation of the boundaries of image for processing is related to types of the images. As it can be seen in figure 15, the gray scale of the defects is closer to the gray value of the surrounded area. Although two defects were detected,

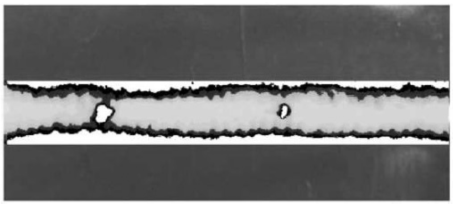

Figure 14: Applying histogram specification

Figure 15: Applying the Threshold (binary image)

but it seems that the right hand defect is less than the main defect, because its boundary pixels of the defect have the light gray colors. Therefore, it is suggested that the surrounding area of each defect is specified separately and processing is performed on that area. Pre-processing and algorithms of image improvement significantly influence on the results of the detected defects. Most defects can be detected successively using mentioned algorithms. However, the change in the threshold level may trivially change the form of the detected defects but the general form of defects does not change. In this study, an advanced image-based system for automatic evaluation of radiographic welding defects is introduced. To test the system, 400 radiographic films were used in 4 different groups, each with 100 films and each group containing 10 duplicate images. It should be noted that the Interpreter has also been used to classify films in these groups. The groups used are: no defect, one defect, two defects and images with more than two defects. The performance of the system in processing images was 100% flawless with the interpreter being the same, although the system was only able to identify 3 similar images. In the group of images with one defect, 97% corresponded to the interpreter, and in the group of images with two defects, this correspondence was 100%. In the group of films with more than two defects, the system performed better than the interpreter, and in an image in which the interpreter identified three defects, the system identified four defects. In addition, in identifying duplicate images in groups with one defect, the result is 100%, for two defects 90% and for more than two defects 100%.

The results of this test have been presented in table 1. In addition, the proposed system fixes the lack of details which have been created due to darkness of the film and its reason is the lack of saving films on magnetic tools.

Table 1: Specifications of the studied films

Image group	**Number of images for testing**	**Number of defective images identified by the expert**	**Number of defective images detected by the system**	**Number of similar images detected by the system**	**Percentage of agreement of the interpreter's ideas with system**	**Percentage of identifying similar images**
Films without defect	100	0	0	3	100	30
Films with one defect	100	100	97	10	97	100
Films with two defects	100	100	100	9	100	90
Films with more than two defects	100	100	100	10	100	100

In the case of using complementary information such as welding hour, welder's code, climatic region, temperature of environment, the rate of humidity, and wind speed, etc., and creating a database using original images and processed images, we can select the best welder in necessary times so that the minimum errors exist in welding process. In addition, we can extract the circumference and area of the defects by standardizing the images.

References

[1] A. Baştürk and E. Günay, *Efficient edge detection in digital images using a cellular neural network optimized by differential evolution algorithm*, Expert Syst. Appl. **36** (2009), no. 2, 2645–2650.

[2] K.J. Batenburg and J. Sijbers, *Optimal threshold selection for tomogram segmentation by projection distance minimization*, Medical Imaging, IEEE Trans. Medical Imag. **28** (2009), no. 5, 676–686.

[3] F.C. Billingsley, *Applications of digital image processing*, Appl. Optics **9** (1970), no. 2, 289–299.

[4] M. Carrasco and D. Merry, *Automatic multiple view inspection using geometrical tracking and feature analysis in aluminum wheels*, Machine Vision Appl. **22** (2011), 157–170.

[5] A. Ebrahimi, K. Mirzaei and A. Latif, *Parallel techniques for detecting defects in radiographic evaluation of oil and gas pipelines using image processing*, Indian J. Fund. Appl. Life Sci. **5** (2015), no. S2, 1598–1609.

[6] A. Ebrahimi, K. Mirzaei and A. Latif, *A hybrid approach for categorizing images based on complex networks and neural networks*, Int. J. Electr. Comput. Eng. **12** (2022), no. 2, 1795–1806.

[7] J. Fan, D.K. Yau, A.K. Elmagarmid and W.G. Aref, *Automatic image segmentation by integrating color-edge extraction and seeded region growing*, IEEE Tran. Image Process. **10** (2001), no. 10, 1454–1466.

[8] R.C. Gonzalez and R.E. Woods, *Digital image processing: Introduction*, Pearson International Edition, 2002.

[9] R.C. Gonzalez, R.E. Woods and S.L. Eddins, *Digital image processing using MATLAB*, Knoxville: Gatesmark Publishing, 2009.

[10] S. Jagannathan, *Automatic inspection of wave soldered joints using neural networks*, J. Manuf. Syst. **16** (1997), no. 6, 389–398.

[11] T.-H. Kim, T.-H. Cho, Y.S. Moon and S.H. Park, *Visual inspection system for the classification of solder joints*, Pattern Recogn. **32** (1999), 565–575.

[12] T.W. Liao, *Improving the accuracy of computer-aided radiographic weld inspection by feature selection*, NDT E Int. **41** (2009), no. 4, 229–239.

[13] R. Myers, R.C. Wison and E.R. Hancock, *Bayesian graph edit distance*, IEEE Trans. Pattern Anal. Machine Intell. **22** (2000), no. 6, 628–635.

[14] R. Ohlander, K. Price and D.R. Reddy, *Picture segmentation using a recursive region splitting method*, Comput. Graph. Image Process. **8** (1978), no. 3, 313–333.

[15] G. Senthil Kumar, U. Natarajan and S. Ananthan, *Vision inspection system for the identification and classification of defects in MIG welding joints*, Int. J. Adv. Manuf. Tech. **61** (2012), no. 9, 923–933.

[16] H.I. Shafeek, E.S. Gadelmawla, A.A. Abdel-Shafy and I.M. Elewa, *Automatic inspection of gas pipeline welding defects using an expert vision system*, NDT E Int. **37** (2004), no. 4, 301–307.

[17] J. Tang, B. Jiang, C.-C. Chang and B. Luo, *Graph structure analysis based on complex network*, Digital Signal Process. **22** (2012), no. 5, 713–725.